Applied and Environmental Microbiology

NhaR, LeuO and H-NS are part of an expanded regulatory network for ectoine biosynthesis expression

Katherine E. Boas Lichty, Gwendolyn J. Gregory, E. Fidelma Boyd*

Department of Biological Sciences, University of Delaware, Newark, DE, 19716

Corresponding author*
E. Fidelma Boyd
Department of Biological Sciences
341 Wolf Hall, University of Delaware
Newark, DE 19716
Phone: (302) 831-1088. Fax: (302) 831-2281 Email: fboyd@udel.edu

Keywords: Ectoine biosynthesis regulation, *Vibrio*, LeuO, NhaR, H-NS, ToxR

Abstract

Bacteria accumulate compatible solutes, to maintain cellular turgor pressure when exposed to high salinity. In the marine halophile *Vibrio parahaemolyticus*, the compatible solute ectoine is biosynthesized *de novo*, which is energetically more costly than uptake; therefore, tight regulation is required. To uncover novel regulators of the ectoine biosynthesis *ectABC-asp_ect* operon, a DNA affinity pulldown of proteins interacting with the *ectABC-asp_ect* regulatory region was performed. Mass spectrometry analysis identified, amongst others, three regulators: LeuO, NhaR, and the nucleoid associated protein H-NS. In-frame non-polar deletions were made for each gene and P_{ectA}-*gfp* promoter reporter assays were performed in exponential and stationary phase cells. P_{ectA}-*gfp* expression was significantly repressed in the Δ*leuO* mutant and significantly induced in the Δ*nhaR* mutant compared to wild type, suggesting positive and negative regulation, respectively. In the Δ*hns* mutant, P_{ectA}-*gfp* showed increased expression in exponential phase cells, but no change compared to wild type in stationary phase cells. To examine whether H-NS interacts with LeuO or NhaR at the ectoine regulatory region, double deletion mutants were created. In a Δ*leuO*/Δ*hns* mutant, P_{ectA}-*gfp* showed reduced expression, but significantly more than Δ*leuO* suggesting H-NS and LeuO interact to regulate ectoine expression. Whereas Δ*nhaR*/Δ*hns* had no additional effect as compared to Δ*nhaR* suggesting NhaR regulation is independent of H-NS. To examine *leuO* regulation further, a P_{leuO}-*gfp* reporter analysis was examined that showed

significantly increased expression in the Δ*leuO*, Δ*hns* and Δ*leuO*/Δ*hns* mutants as compared to wild type, indicating both are repressors. Growth pattern analysis of the mutants in M9G 6%NaCl, showed growth defects compared to wild type, indicating that these regulators play an important physiological role in salinity stress tolerance.

Importance: Ectoine is a commercially used compatible solute that acts as a biomolecule stabilizer because of its additional role as a chemical chaperone. A better understanding of how the ectoine biosynthetic pathway is regulated in natural bacterial producers can be used to increase efficient industrial production. The *de novo* biosynthesis of ectoine is essential for bacteria to survive osmotic stress when exogenous compatible solutes are absent. This study identified LeuO as a positive regulator and NhaR as a negative regulator of ectoine biosynthesis and also showed that similar to enteric species, LeuO is an anti-silencer of H-NS. In addition, defects in growth in high salinity among all the mutants suggest that these regulators play a broader role in the osmotic stress response beyond ectoine biosynthesis regulation.

57 **Introduction**

58 When bacteria are exposed to high salinity conditions, an efflux of water across the
59 osmotic gradient occurs lowering cellular turgor pressure (1-5). The initial short-term
60 response to osmotic up shock is the uptake of potassium (K+), which is accompanied by
61 glutamate accumulation in Gram-negative bacteria to maintain electro neutrality. This
62 is the short-term strategy because high concentrations of K+ have deleterious effects on
63 cellular processes (1, 2, 6, 7). The long term response to increased osmotic stress is
64 characterized by the uptake or biosynthesis of compatible solutes, which are small
65 organic molecules that provide osmotic protection by helping to maintain the turgor
66 pressure of the cell and can be accumulated to extremely high intracellular
67 concentrations (3, 8, 9).

68 The compatible solute ectoine was initially discovered to provide osmotic protection in
69 anoxygenic phototrophs (10), but subsequent analysis showed that it functions as a
70 compatible solute in numerous Gram-negative and Gram-positive bacteria (reviewed in
71 (3, 8, 11-14), which included many members of the family *Vibrionaceae* (15-19).
72 Accumulation to very high intracellular concentrations without interfering with
73 molecular processes is a hallmark of compatible solutes. Additionally, ectoine acts as a
74 chemical chaperone through the stabilization of proteins, thus it is an important
75 compound for commercial uses in medicine and cosmetics to stabilize biomolecules
76 against factors such as heating, freezing, desiccation, and UV radiation (20-23).

77 Therefore, understanding the regulation of the ectoine biosynthetic pathway is
78 important to increase efficient industrial production using natural bacterial producers
79 (24).

80 Biosynthesis of ectoine (1,4,5,6-tetrahydro-2-methyl-4-pyrimidinecarboxylic acid) is *de*
81 *novo* from L-aspartic acid, and performed by the evolutionarily conserved operon
82 *ectABC*, which encodes the EctA, EctB, and EctC proteins (25-27) (**Fig. S1**). In many
83 species an aspartokinase (*asp_ect*) is clustered with the ectoine biosynthesis operon,
84 which converts aspartic acid to β-aspartyl phosphate, which is then converted to L-
85 aspartate-β-semialdehyde by aspartate semialdehyde dehydrogenase (Asd). This
86 intermediate from the aspartic acid pathway is incorporated into the ectoine
87 biosynthesis pathway when it is converted to L-2,4-diaminobutyrate by EctB (L-2,4-
88 diaminobutyrate transaminase). EctA (L-2,4-diaminobutyrate N^{γ}-acetyltransferase) then
89 acetylates this product to form N^{γ}-acetyldiaminobutyrate. The final step to produce
90 ectoine is a cyclic condensation reaction performed by EctC (L-ectoine synthase) (13,
91 27).

92 In some species, clustered with the ectoine biosynthesis operon is *ectR*, a MarR-type
93 regulator shown to repress transcription of the ectoine operon (24, 28-30). Among
94 *Vibrionaceae*, an *ectR* homolog is present only in *Aliivibrio* species (31, 32). Previous
95 studies in *V. parahaemolyticus* and *V. cholerae* showed that *ectABC-asp_ect* transcription
96 was repressed in low salinity by another MarR-type regulator named CosR (17, 31, 33).

97 CosR from *V. parahaemolyticus* showed 31% amino acid identity to *Aliivibrio fischeri* EctR,
98 with less than 60% query coverage and does not cluster with *ectABC-asp_ect*, but is
99 located elsewhere in the genome (31). The quorum sensing master regulators AphA and
100 OpaR activate and repress expression of *ectABC-asp_ect*, respectively in *V.*
101 *parahaemolyticus* (17). AphA and OpaR also regulate expression of CosR, creating a
102 tightly controlled feed-forward loop for ectoine expression across the growth curve (17).

103 In this study, we set out to identify novel regulators of the ectoine biosynthesis genes by
104 performing a DNA affinity chromatography pulldown using the regulatory region of
105 the *ectABC-asp_ect* operon. We identified numerous candidates and selected the
106 regulators LeuO, NhaR, OmpR, TorR, and the nucleoid associated protein (NAP) H-NS
107 to examine further. We constructed in-frame nonpolar deletions in each gene. These
108 regulators play a role in the regulation of the ectoine biosynthesis genes based upon
109 P_{ectA}-*gfp* expression reporter assays. In addition, analysis of double mutants Δ*leuO*/Δ*hns*
110 and Δ*nhaR*/Δ*hns* showed that H-NS interacted with LeuO but not NhaR to control
111 ectoine gene expression. Importantly, when these deletion mutants were grown under
112 high salinity conditions a growth defect was observed, suggesting that the regulators
113 NhaR, LeuO, and H-NS are physiologically important for growth in high salinity
114 conditions.

115

116 **Results**

117 **Ectoine is biosynthesized in cells grown in M9G 3%NaCl, but absent in M9G**
118 **1%NaCl.** To confirm *V. parahaemolyticus de novo* ectoine biosynthesis is a response to
119 increased salinity, ^{1}H nuclear magnetic resonance spectroscopy (^{1}H-NMR) at 600MHz in
120 the presence of deuterium oxide as the solvent was performed. Ethanol extracts of *V.*
121 *parahaemolyticus* wild type cells grown overnight at 37°C in minimal medium
122 supplemented with glucose (M9G) with either 1%NaCl or 3%NaCl were used to obtain
123 ^{1}H-NMR spectra (**Fig. S2A**). Peaks corresponding to the hydrogen atoms of ectoine are
124 labeled and were present in M9G 3%NaCl extracts but were not detectable in M9G
125 1%NaCl extracts as previously shown (15) (**Fig. S2A**). In addition to intracellular
126 accumulation of ectoine, we also wanted to demonstrate that *ectABC-asp_ect* expression
127 is increased in M9G 3%NaCl compared to 1% NaCl. A transcriptional reporter assay
128 was performed, where *gfp* was placed under the control of the ectoine regulatory region
129 (P_{ectA}-*gfp*). The expression was examined in wild type cells grown in either M9G 1%NaCl
130 or M9G 3%NaCl by measuring the specific fluorescence of P_{ectA}-*gfp* as a cumulative
131 readout of *ectA* transcription (**Fig. S2B**). The observed level of specific fluorescence of
132 P_{ectA}-*gfp* was significantly increased in M9G 3%NaCl (4.0-fold) relative to that of cells
133 grown in M9G 1%NaCl (**Fig. S2B**).

134 **Identification of putative regulators of the ectoine biosynthesis operon.** With the
135 knowledge that ectoine is present in cells grown in M9G 3%NaCl, we performed a

136 promoter pulldown under this growth condition. A promoter pulldown was performed
137 using a 5′-biotin tagged 323-bp DNA fragment of the *ectABC-asp_ect* regulatory region
138 bound to streptavidin beads. As a negative control DNA probe, the coding region of the
139 *ectB* gene was used. To identify novel regulators of ectoine biosynthesis, we grew cells
140 to mid-exponential phase in M9G 3%NaCl and subsequent cell lysate was incubated
141 with DNA probe-coated beads. Bound proteins were then eluted using a stepwise NaCl
142 gradient and separated with SDS-PAGE gel (**Fig. S3A**). Bands that were present in the
143 target lanes, but not present in the *ectB* negative control lanes were selected for analysis
144 via mass spectrometry (**Fig. S3B**). The proteins identified with mass spectrometry
145 analysis were aligned to the *V. parahaemolyticus* genome and sorted by gene class and
146 ranked by score (**Table S1**). The mass spectrometry score is the combined sum of all
147 scores for an observed spectra that can be matched to an individual peptide. The higher
148 the score the more confident the match to the specified peptide. Candidate proteins of
149 interest that belonged to the transcriptional regulator gene class were selected. These
150 candidate proteins are described in Table S1 and include homologs of regulators NhaR
151 (VP0527), OmpR (VP0154), and TorR (VP1032). NhaR and OmpR were shown in
152 *Escherichia coli*, which does not produce ectoine, to be involved in the osmotic stress
153 response (34-39). *V. parahaemolyticus* NhaR shows 62%, OmpR 84%, and TorR 57%
154 amino acid identities to homologs in *E. coli*. NhaR, OmpR, and TorR have not been
155 examined in *Vibrio* species. An additional regulators of interest, LeuO (VP0350), a LysR-

156 type regulator and H-NS (histone-like nucleoid structuring) protein were also examined
157 further. In *V. parahaemolyticus*, LeuO was previously shown to be positively regulated
158 by ToxR and is essential for acid stress tolerance (40, 41). H-NS in *E. coli* and *Salmonella*
159 *enterica*, is a universal silencer of gene expression (42-47). In addition, an *E. coli* study by
160 Shimada and colleagues identified 140 LeuO-binding sites with over 90% of these sites
161 also showing H-NS binding. Further studies have shown that LeuO plays a significant
162 role as an antagonist of H-NS gene silencing (42, 48, 49). While not chosen for
163 examination in this study, two additional regulators did stand out for possible future
164 analysis, VPA0036 (accession number Q87K62) and VP0489 (accession number Q87SD5)
165 (**Table S1**). VPA0036 gave a high score, but is annotated as a hypothetical protein with
166 no conserved domains. HHPred analysis uncovered a putative N-terminal winged-helix
167 protein domain with a probability of 96.53% and E-value 0.016. VP0489 is annotated as
168 an aerobic respiration control protein FecA and ArcA a two-component system
169 response regulator.

170 As a proof of concept for the pulldown, LeuO and NhaR proteins were purified and
171 visualized on SDS-PAGE gels showing an expected 36.2 kDa LeuO protein and a 33.9
172 kDa NhaR protein (**Fig. S4**). Electrophoretic mobility shift assays (EMSAs) were
173 performed first using the 323-bp regulatory region of *ectABC-asp_ect* as a DNA probe
174 (**Fig. S5A**). For the LeuO EMSA, we used the regulatory region of the *leuO* gene as a
175 positive control and show binding in a concentration dependent manner for this and

176 also for the P*ectA* probe 1 (**Fig. S5B**). Binding of NhaR to P*ectA* was also confirmed in
177 the EMSA (**Fig. S5C**). To examine binding of LeuO and NhaR further, probe 1 was
178 divided into three similarly sized probes P*ectA* 1A, 1B and 1C. Purified protein LeuO
179 showed band shifts for probe 1A and a complete shift for probe 1C (**Fig. S5D**). For
180 NhaR all three probes showed shifts in a concentration dependent manner (**Fig. S5E**).

181 **P*ectA-gfp* reporter assays shows differential expression in Δ*leuO*, Δ*nhaR*, Δ*ompR* and**
182 **Δ*torR* mutants**. To examine the role of *leuO*, *nhaR*, *ompR*, and *torR* candidate regulators,
183 we performed GFP reporter assays using a reporter plasmid where *gfp* was under the
184 control of the ectoine regulatory region (P_{ectA}-*gfp*). This reporter plasmid was
185 transformed into wild type or in-frame non-polar mutants of Δ*leuO*, Δ*nhaR*, Δ*ompR*, and
186 Δ*torR*. Cultures were grown overnight in M9G 3% NaCl and relative fluorescence
187 intensity (RFU) was measured. Specific fluorescence was calculated by dividing RFU by
188 OD. From this analysis, the relative fluorescence (RFU) measured in the Δ*leuO* mutant
189 background was 1.7-fold reduced as compared to wild type (**Fig. 1**). This data suggests
190 that LeuO is an activator of *ectABC-asp_ect*. The relative fluorescence measured in a
191 Δ*nhaR* background was significantly increased 1.8-fold as compared to wild type,
192 suggesting that NhaR is a repressor of *ectABC-asp_ect* (**Fig. 1**). P_{ectA}-*gfp* expression in the
193 Δ*ompR* (1.3-fold) and Δ*torR* (1.4-fold) mutants were also increased as compared to wild
194 type, but not to the same level as NhaR.

195 **LeuO and H-NS interplay to control P_{ectA}-*gfp*.** In *E. coli* and *V. cholerae*, H-NS has been
196 shown to interact with LeuO in both cooperative and antagonistic relationships at
197 different gene loci (42, 50-53). Therefore, we wanted to examine whether H-NS and
198 LeuO interacted at the *ectABC-asp_ect* regulatory region. We constructed an in-frame
199 non-polar Δ*hns* mutant and a double Δ*leuO*/Δ*hns* mutant. In exponential phase cells (OD
200 ~ 0.4), P_{ectA}-*gfp* in the Δ*leuO* mutant showed significant reduced expression, and in the
201 Δ*hns* mutant expression was significantly increased (**Fig. 2A**). However, in the
202 Δ*leuO*/Δ*hns* double mutant P_{ectA}-*gfp* expression was reduced, but not to the same level as
203 the Δ*leuO* single mutant (**Fig. 2A**). In stationary phase cells (OD ~ 1.0), P_{ectA}-*gfp* relative
204 fluorescence was similar to exponential cells in all strains except the Δ*hns* mutant, which
205 was similar to wild-type (**Fig. 2B**). These data indicate interplay between both LeuO
206 and H-NS to control ectoine gene expression with LeuO playing an anti-silencer role.

207 To further investigate the relationship between LeuO and H-NS in *V. parahaemolyticus*, a
208 *gfp*-expressing reporter plasmid under the control of the LeuO regulatory region (P_{leuO}-
209 *gfp*) was constructed. Relative fluorescence was measured in cells grown to OD ~1.0 in
210 M9G 3%NaCl in wild type, Δ*leuO*, Δ*hns*, Δ*leuO*/Δ*hns*, and Δ*toxR*. When compared to
211 wild type, P_{leuO}-*gfp* expression in the Δ*hns* mutant showed a 4.0-fold increased relative
212 fluorescence indicating that H-NS is a repressor of *leuO* expression (**Fig. 3**). P_{leuO}-*gfp*
213 expression was 2.4-fold higher in Δ*leuO* and 2.8-fold higher in Δ*leuO*/Δ*hns* when
214 compared to wild type. In *V. parahaemolyticus*, ToxR is a positive regulator of *leuO*

215 expression (40, 54, 55) and this was confirmed in this reporter assay, with Δ*toxR*
216 showing reduced P_{leuO}-*gfp* (1.8-fold) expression when compared to wild type (**Fig. 3**).
217 These data indicate that both H-NS and LeuO are repressors of *leuO* expression and in
218 the absence of both negative regulators other proteins such as ToxR are likely able to
219 access the regulatory region.

220 **H-NS and LeuO are important for growth in high salinity.** To assess whether the
221 deletions of *leuO* and *hns* have a physiological effect, we examined the ability of *V.*
222 *parahaemolyticus* wild type, Δ*leuO*, Δ*hns*, and Δ*leuO*/Δ*hns* mutants to grow in M9G 1%
223 NaCl, 3%NaCl, or 6%NaCl at 37°C. In M9G 1%NaCl and 3%NaCl, there were no
224 significant growth defects observed among most strains, with the exception of Δ*leuO*,
225 which reached a lower final OD (0.44) as compared to wild type (0.57) (**Fig. S6A, 6B**).
226 Growth in M9G 6%NaCl showed the wild type and Δ*hns* had a 5 h lag phase, but the
227 Δ*hns* mutant reached a lower final OD (0.37) as compared to wild type (0.54) (**Fig. 4).**
228 The Δ*leuO* mutant had a lag phase of 6 h and Δ*leuO*/Δ*hns* had a 13 h lag phase. In
229 addition, the double deletion mutant had a final OD_{595} of 0.2, which was significantly
230 less than wild type with final OD of 0.54 (**Fig. 4**). Complementation of Δ*leuO* with
231 pBA*leuO* and Δ*hns* with pBA*hns*, restored growth to wild type levels (**Fig. 4**). However,
232 we were unable to complement the double mutant with either pBA*leuO* or pBA*hns*.
233 Overall, these data demonstrate that both LeuO and H-NS play a significant role in the
234 osmotic stress response and are required for optimal growth in high salinity.

235 **NhaR is a negative regulator of the ectoine biosynthesis operon.** Next, we considered
236 whether there was interplay between NhaR and H-NS in the regulation of *ectABC-ask*.
237 To accomplish this, we examined P_{ectA}-*gfp* in Δ*nhaR*, Δ*hns* and a Δ*nhaR*/Δ*hns* double
238 mutant in M9G 3%NaCl in exponential and stationary phase cells (**Fig. 5**). In
239 exponential cells (~OD 0.4). P_{ectA}-*gfp* expression was higher in Δ*nhaR* (1.8-fold) as
240 compared to wild type confirming NhaR as a negative regulator (**Fig. 5A**). P_{ectA}-*gfp*
241 expression in the Δ*hns* and Δ*hns*/Δ*nhaR* mutants were both similarly increased
242 compared to wild type (**Fig. 5A**). Examination of stationary phase cells (OD ~ 1.0) gave
243 similar results to expression in exponential cells with the exception of Δ*hns*, which
244 showed P_{ectA}-*gfp* expression levels similar to wild type (**Fig. 5B**). Overall, the data
245 suggest that there is no interplay between H-NS and NhaR in ectoine expression
246 because the double mutant was not significantly different than the single mutants.

247 Next, we examined the effect of deleting *nhaR*, *hns*, and *hns*/*nhaR* on growth of *V.*
248 *parahaemolyticus* in high salinity. Growth of the deletion mutants in M9G 1%NaCl and
249 3% NaCl was similar to wild type indicating no overall defect (**Fig. S6C, D**). However,
250 Δ*nhaR*, Δ*hns*, and Δ*hns*/Δ*nhaR* mutants grown in M9G 6%NaCl, reached a final OD_{595} of
251 0.37, 0.36, and 0.38 respectively as compared to wild type OD_{595} of 0.5 (**Fig. 6**).
252 Complementation of Δ*nhaR* with pBA*nhaR* restored growth to wild type levels (**Fig. 6**).
253 These data indicates that there is a growth defect in high salinity for Δ*nhaR*, but deletion
254 of *hns* does not contribute further to this defect. This supports the expression data that

255 NhaR and H-NS do not interact to control ectoine expression. The data does indicate
256 that NhaR is important for high salinity tolerance.

257 **Discussion**

258 The accumulation of compatible solutes occurs either via uptake or biosynthesis and in
259 *V. parahaemolyticus* there are six transporters and two biosynthesis operons for
260 compatible solutes present (19, 56). The biosynthesis of the compatible solute ectoine
261 and not glycine betaine was previously shown to be essential for *V. parahaemolyticus*
262 survival in high salinity (15). However, ectoine biosynthesis is costly as it drains
263 intracellular pools of metabolites such as aspartic acid and multiple regulators that
264 provide tight control are needed (57).

265 In this study, we identified several new regulators of ectoine biosynthesis (**Fig. 7**). We
266 found that NhaR acted as a repressor of ectoine biosynthesis. However, deletion of this
267 repressor, showed a defect when grown under high salinity conditions (6% NaCl). This
268 could be explained by the fact that NhaR is known to regulate genes related to the
269 osmotic stress response outside of ectoine biosynthesis (58-61). In *E. coli*, *nhaR* is present
270 in an operon with *nhaA*, which encodes a Na+/H+ antiporter. NhaR was shown to
271 activate transcription of *nhaA*, which is induced in high salt and alkaline pH and is
272 essential for survival under these conditions. It was also suggested that NhaR is a
273 sensor and transducer of Na+ because the presence of Na+ alters the contact points

274 between NhaR and the *nhaA* regulatory region (62). A homolog of *nhaA* is present in *V.*
275 *parahaemolyticus*, and thus may also be activated by NhaR, which could explain the
276 growth defect in high salinity for the *V. parahaemolyticus ΔnhaR* mutant.

277 Our data also established that LeuO is a positive regulator of ectoine biosynthesis gene
278 expression and H-NS acts as a gene silencer. The analysis of a double Δ*leuO*/Δ*hns*
279 mutant suggested that LeuO also likely plays a role as an anti-silencer of H-NS at this
280 locus. In addition, we found that LeuO and H-NS both act as repressors of *leuO* in *V.*
281 *parahaemolyticus*, further supporting the interaction between these two regulators.

282 LeuO was first identified as a LysR-type regulator and shown to positively regulate the
283 *leuABCD* leucine synthesis operon in *Salmonella enterica* (63, 64). Subsequently,
284 chromatin-immunoprecipitation-on-chip analysis showed 178 LeuO binding sites in *S.*
285 *enterica*, indicating its role as a global regulator (65). H-NS was also shown to be a global
286 regulator in this species and in *E. coli*, silencing the transcription of a large number of
287 horizontally acquired genes (46, 47, 66). In *V. parahaemolyticus*, LeuO was first named
288 CalR as it was negatively regulated by calcium (41). LeuO was shown to positively
289 regulate *ompU*, which encodes an outer membrane porin important for acid stress (**Fig.**
290 **7**) (40). Additionally, the global regulator ToxR was shown to be a positive regulator of
291 *leuO* expression and deletion of either *leuO* or *toxR* resulted in a growth defect in acid
292 conditions (40). In our study, *leuO* showed significantly increased expression in the
293 Δ*leuO* mutant whereas in the Δ*toxR* mutant *leuO* expression was reduced showing it is

294 an activator (**Fig. 7**). In *V. vulnificus*, H-NS was shown to repress *leuO* by binding to sites
295 that overlap with ToxR and LeuO binding sites (67, 68). Our data also showed that *leuO*
296 is an auto-repressor and that H-NS represses *leuO* in *V. parahaemolyticus*, which is likely
297 using a similar regulatory mechanism to that in *V. vulnificus* (**Fig. 7**). Our growth data
298 showed that deletion of either *leuO* or *hns* resulted in defects when grown at high
299 salinity and a double Δ*leuO*/Δ*hns* mutant showed a severe growth defect that was more
300 pronounced than either of the single mutants. The observed defects in high salinity
301 suggests a larger role for both regulators in the osmotic stress response. The more
302 pronounced growth defect observed for Δ*leuO*/Δ*hns* reinforces the hypothesis that these
303 proteins interact at other loci important for increased salinity toleranace.

304 **Methods**

305 **Bacterial strains, media and culture conditions**. All strains and plasmids used in this
306 study are listed in Table S2. *V. parahaemolyticus* RIMD2210633, a streptomycin-resistant
307 clinical isolate, was used in this study as the wild-type (WT) strain (69, 70). Unless
308 stated otherwise, *V. parahaemolyticus* was grown in either lysogeny broth (LB; Fisher
309 Scientific, Fair Lawn, NJ) with 3% (wt./vole) NaCl (LB 3%) or M9 minimal media (47.8
310 mM Na_2HPO_4, 22 mM KH_2PO_4, 18.7 mM NH_4Cl, 8.6 mM NaCl; Sigma Aldrich)
311 supplemented with 2 mM $MgSO_4$, 0.1 mM $CaCl_2$, 20 mM glucose as the sole carbon
312 source (M9G) and 3% (wt/vol) NaCl at 37°C. *E. coli* strains were grown in either LB
313 supplemented with 1% (wt/vol) NaCl (LB1%) or M9G supplemented with 1% (wt/vol)

314 NaCl. The strain *E. coli* β2155 *λpir* strain is a diaminopimelic acid (DAP) auxotrophic
315 strain and was grown with 0.3 mM DAP (71). All strains were grown at 37°C with
316 aeration. Antibiotics were added to growth media at the following concentrations as
317 necessary: ampicillin (Amp), 100 μg/mL; chloramphenicol (Cm), 12.5 μg/mL;
318 tetracycline (Tet), 1 μg/mL; kanamycin (Km), 50 μg/mL.

319 **Preparation of cellular extracts and proton nuclear magnetic resonance (^{1}H-NMR)**.
320 Wild-type *V. parahaemolyticus* was grown overnight at 37°C in either M9G 1% NaCl or
321 M9G 3%NaCl. Stationary phase cells were then pelleted and washed twice with 1XPBS.
322 Three freeze-thaw cycles were performed with the cell pellets to increase lysis, and the
323 cells were then suspended in 750 μL ethanol. Debris was pelleted by centrifugation, and
324 the ethanol solution was transferred to a clean tube and evaporated under vacuum.
325 Then deuterium oxide (D_2O) was used to resuspend the pellet, and insoluble material
326 was removed by centrifugation. The solution was then transferred to a 5-mm NMR tube
327 for analysis on a Bruker AVANCE 600NMR spectrometer at a proton frequency of
328 600.13 MHz with a sweep of 12,376 Hz and a relaxation delay of 5 s. Sixteen scans were
329 co-added for each spectrum.

330 **DNA-Affinity Pulldown.** DNA-affinity chromatography pulldown was performed as
331 previously described (72-74). The bait DNA primers were designed to amplify the 323-
332 bp regulatory region of *ectA* (VP1722) with a biotin moiety added to the 5′ end. A 327-
333 bp negative-control bait DNA probe was amplified from a coding region of *ectB*

334 (VP1721), which was also labeled with a biotin moiety at the 5′ end. Both probes were
335 amplified using Phusion HF polymerase (New England Biolabs) PCR. Ten reactions
336 were completed for each probe and then pooled and purified using an ethanol
337 extraction technique (75). The pulldown was completed twice, once after growth in non-
338 inducing conditions (LB3%) and once after growth in inducing conditions (M9G3%) in
339 an effort to obtain both positive and negative regulators of the ectoine biosynthesis
340 operon. The wild-type strain was grown overnight in LB3%, cells were pelleted and
341 washed two times with 1XPBS and diluted 1:50 into 500 mL of LB3% or M9G3%. The
342 cultures were then grown to an OD_{595} of 0.5, pelleted and stored overnight at -80°C. The
343 pellet was then suspended in 1.5 mL Fast-Break lysis buffer (Promega, Madison, WI)
344 with 1 mM PMSF, 0.5 mM benzamidine, 0.1 μg/mL lysozyme and incubated for 30 min.
345 at room temperature. The cells were then sonicated on ice at 30% pulse amplitude for 15
346 seconds with 1 min. rest, and this was repeated 5 times. The cell lysate was then
347 clarified by centrifugation for 30 min. at 4°C. The cell lysate was precleared with
348 streptavidin DynaBeads (Thermo Scientific, Waltham, MA) to remove nonspecific
349 protein-bead interactions.

350 Streptavidin M280 DynaBeads (ThermoFisher) were then incubated two times with 10
351 μg of biotinylated probe for 20 min. The precleared cell lysate was then incubated for 30
352 min. with the bait-coated beads at room temperature with constant rotation in the
353 presence of 100 μg sheared salmon sperm DNA as a non-specific competitor. This was

354 completed twice with washes in between. Protein candidates were then eluted from the
355 bait DNA-bead complex with a stepwise NaCl gradient (100 mM, 200 mM, 300 mM, 500
356 mM, 170 mM, and 1 M). Next, 6X SDS and 1 mM β-mercaptoethanol (BME) was added
357 to elution samples which were then boiled at 95°C for 5 min. Samples were then
358 separated using a 12% SDS-PAGE and visualized using the Pierce Silver Stain Kit
359 (ThermoFisher). The P_{ectA} bait and *ectB* negative control were loaded next to each other
360 in order of increasing NaCl concentrations. Bands that were present in the P_{ectA} bait but
361 not the negative control lanes were excised, de-stained, and digested with trypsin
362 following the standard procedure for mass spectrophotometry preparation with C18
363 ZipTips (Fisher Scientific, Fair Lawn, NJ). The samples were then individually analyzed
364 with a Q-exactive Orbitrap mass spectrometer with nano-flow electrospray (Thermo).
365 Proteins were subsequently identified using Proteome Discover 2.1 software.

366 **Protein Purification**. Protein were purified as previously described (76). The full-length
367 genes for *leuO* (VP0350) and *nhaR* (VP0527) were cloned into a pET-28a(+) vector with a
368 C-terminal histidine tag, transformed into *E. coli* Dh5α, purified, and sequenced. These
369 vectors pET*leuO* and pET*nhaR* were then transformed into *E. coli* BL21 (DE3) cells, and
370 expression was induced with 0.5mM IPTG at 0.4 OD_{595} and then cells were grown
371 overnight at 25°C. Cells were then pelleted and resuspended with lysis buffer (50 mM
372 sodium phosphate, 200 mM NaCl, 20 mM imidazole, pH 7.4, 1.0 mM
373 phenylmethanesulfonyl fluoride, 0.5 mM benzamidine) and lysed via sonication. Debris

374 was pelleted, and supernatant applied to an IMAC column packed with HisPur Ni-
375 NTA resin (ThermoFisher) that was equilibrated with column buffer (50 mM sodium
376 phosphate, 200 mM NaCl, 20 mM imidazole, pH 7.4). The column was washed with
377 buffer containing increasing concentrations of imidazole (20mM – 100mM) to remove
378 any contaminants. His-tagged proteins were eluted using 500mM imidazole and then
379 dialyzed overnight at 4°C in sodium phosphate buffer to remove any excess salts.
380 Samples of supernatant and each flow through, wash, and elution were analyzed via
381 SDS-PAGE gel to assess protein purity and verify purification.

382 **Electrophoretic mobility shift assay**. DNA fragments were designed as outlined in
383 Table S3, to encompass the entire region (322-bp) or sections of the ectoine biosynthesis
384 regulatory region (125, 137, 106-bp). The concentration of purified protein (LeuO-His or
385 NhaR-His) was determined using the Bradford Assay, and LeuO (0 to 2.175 uM) or
386 NhaR (0 to 2.175 uM) was incubated for 20 minutes with 30 ng of each DNA fragment
387 in a binding buffer (10 mM Tris [pH 7.4 at 4°C], 150 mM KCl, 0.1 mM dithiothreitol, 0.1
388 mM EDTA [pH 8.0], 5% polyethylene glycol). The reactions were then loaded (10 μL) on
389 a 6% native acrylamide gel (pre-run 200V for 2 hours at 4°C) and run for 2 hours at 4°C
390 (200V) in 0.5X TBE running buffer. To visualize, gels were stained in an ethidium
391 bromide bath for 15 minutes.

392 **Mutant strain construction**. In-frame deletion mutants of *nhaR* (VP0527), *torR*
393 (VP1032), and *hns* (VP1133), were designed as previously described via allelic exchange

394 (17). A truncated region of the *nhaR* (15-bp of the 891-bp), *torR* (54-bp of the 714-bp),
395 and *hns* (33-bp of the 408-bp) genes was generated using the primers in Table S3. The
396 truncated products were then ligated with the suicide vector pDS132 using the Gibson
397 assembly protocol and transformed into *E. coli* Dh5α (77, 78). The resulting plasmids
398 pDSΔ*nhaR*, pDSΔ*torR*, and pDSΔ*hns* were purified and transformed into *E. coli* β2155
399 λ*pir* (diaminopimelic acid auxotroph), followed by conjugation and homologous
400 recombination into the *V. parahaemolyticus* RIMD2210633 genome. Single crossover of
401 the plasmids into the genome were selected for by plating onto chloramphenicol (CM)
402 and screened via PCR for a truncated allele. To induce a double-crossover event, the
403 single-cross strain was grown overnight in the absence of CM, leaving behind either the
404 truncated allele or the wild-type allele. The cultures were spread on 10% sucrose plates,
405 and healthy colonies were screened for double-crossover and gene truncation; colonies
406 that contain the plasmid will appear soupy on the plate due to the presence of the *sacB*
407 selectable marker. In-frame deletions were confirmed with sequencing.

408 An in-frame deletion of *ompR* (VP0154) was created in *V. parahaemolyticus* RIMD2210633
409 through splicing by overlap extension (SOE) PCR and homologous recombination (79).
410 Primers were designed to create a 692-bp truncated allele of *ompR* using the primer pair
411 listed in Table S3. This truncated product was ligated into the cloning vector pJET1.2
412 with T4 DNA ligase and transformed into *E. coli* Dh5α λ*pir*. The truncated *ompR* allele
413 was then excised from the pJETΔ*ompR* vector using restriction enzymes (SacI, XbaI) and

414 ligated into the suicide vector pDS132. The pDSΔ*ompR* vector was then transformed
415 into *E. coli* β2155 *λpir* (DAP auxotroph), and the same procedure as described above
416 was completed. Double mutants Δ*leuO*/Δ*hns* and Δ*hns*/Δ*nhaR* were generated by
417 conjugating *E. coli* β2155 *λpir* + pDS*hns* with *V. parahaemolyticus* Δ*leuO* and β2155 *λpir* +
418 pDS*nhaR* with *V. parahaemolyticus* Δ*hns.* The same procedure as described above was
419 carried out to achieve these double deletions. To confirm that the phenotypes observed
420 in the Δ*leuO*, Δ*hns* and Δ*nhaR* mutants were not due to secondary mutations within the
421 genome, the strains were complemented with functional copies of the gene. The coding
422 regions were amplified from *V. parahaemolyticus* RIMD2210633 genome and cloned into
423 the expression vector pBAD33. Then transformation into *E. coli* β2155 was completed
424 for both vectors. The expression vectors, pBAD*leuO*, pBAD*hns*, pBAD*nhaR* were then
425 conjugated into the Δ*leuO*, Δ*hns* and Δ*nhaR* strains.

426 **Transcriptional GFP-reporter assay**. The reporter construct pRUP$_{ectA}$-*gfp* was created
427 previously using the pRU1064 vector, which contains a promoterless *gfp* cassette, as
428 well as Tet and Amp resistance genes (17, 80). Using *E. coli* β2155 *λpir* containing
429 pRUP$_{ectA}$-*gfp*, the reporter plasmid was conjugated into each of the *V. parahaemolyticus*
430 mutant strains Δ*leuO*, Δ*nhaR*, Δ*torR*, Δ*ompR*, Δ*hns*, Δ*leuO*/Δ*hns*, and Δ*hns*/Δ*nhaR.* Strains
431 were grown overnight in LB3% with tetracycline. The cultures were then washed two
432 times with 1XPBS, diluted 1:100 into M9G3% with tetracycline, and grown to OD ~ 0.4
433 or OD ~ 1.0 as indicated. The reporter expression was determined by measuring the

relative fluorescence with excitation at 385 nm and emission at 509 nm in black, clear bottomed 96-well microplates on a Tecan Spark microplate reader with Magellan software (Tecan Systems, Inc., San Jose, CA). Specific fluorescence was calculated by dividing the relative fluorescence units (RFU) by the optical density of each well. At least two biological replicates were performed for each experiment. Statistics were completed either with a Student's T-test or ANOVA followed by Tukey-Kramer Post Hoc test, as designated.

ACKNOWLEDGEMENTS

This research was supported by a National Science Foundation grant (award IOS-1656688) to E.F.B. KBL and GJG were funded in part by a University of Delaware graduate fellowship award and KBL in part by a Chemistry-Biology Interface predoctoral training program grant: 5T32GM008550.

452 **Figure Legends**

453 **Fig. 1**. Expression of a P_{ectA}-*gfp* transcriptional fusion in wild-type (WT) *V.*
454 *parahaemolyticus* Δ*leuO*, Δ*nhaR*, Δ*ompR*, and Δ*torR* mutants. Cultures were grown
455 overnight in M9G 3% NaCl and relative fluorescence intensity (RFU) was measured.
456 Specific fluorescence was calculated by dividing RFU by OD. Mean and standard
457 deviation of three biological replicates are shown. Statistics were calculated using a
458 Student's t-test; (*, $P < 0.05$; ***, $P < 0.001$).

459 **Fig. 2**. Expression of a P_{ectA}-*gfp* transcriptional fusion in wild-type (WT) *V.*
460 *parahaemolyticus* Δ*leuO*, Δ*hns*, and Δ*leuO*/Δ*hns* mutants. Cultures were grown **A**. to OD
461 ~0.4 or **B**. OD ~1.0 in M9G 3%NaCl and relative fluorescence intensity (RFU) was
462 measured. Specific fluorescence was calculated by dividing RFU by OD. Mean and
463 standard deviation of three biological replicates are shown. Statistics were calculated
464 using an ANOVA followed by Tukey-Kramer post hoc test; (***, $P < 0.001$).

465 **Fig. 3.** Expression reporter assays of P_{leuO}-*gfp* transcriptional fusion in *V.*
466 *parahaemolyticus* wild type (WT), Δ*leuO*, Δ*hns*, Δ*leuO*/Δ*hns*, *and* Δ*toxRS* mutants.
467 Cultures were grown to OD ~1.0 in M9G 3%NaCL and relative fluorescence intensity
468 (RFU) was measured. Specific fluorescence was calculated by dividing RFU by OD.
469 Mean and standard deviation of two biological replicates are shown. Statistics were
470 calculated using a Student's t-test; (*, $P < 0.05$; **, $P < 0.005$).

Fig. 4. Growth analysis of Δ*leuO*, *Δhns* and *ΔleuO*/*Δhns* mutants in M9G 6%NaCl. Cells were grown to OD 0.5 in M9G 1%NaCl and then inoculated into M9G 6%NaCl and growth was measured every hour for 24h at 37°C. Mean and standard deviation of two biological replicates are shown. Also shown, complementation of Δ*leuO* with pBA*leuO* and Δ*hns* with pBA*hns*. For all growth curves the area under the curve (AUC) was calculated for each strain and a Student's t-test was performed (*, $P < 0.05$; **, $P < 0.005$; ***, $P < 0.001$).

Fig. 5. Expression of a P_{ectA}-*gfp* transcriptional fusion in wild type (WT) *V. parahaemolyticus*, Δ*nhaR*, Δ*hns*, *and* Δ*hns*/Δ*nhaR* mutants. Cultures were grown **A**. to OD ~0.4 or **B**. OD ~1.0 in M9G 3%NaCl and relative fluorescence intensity (RFU) was measured. Specific fluorescence was calculated by dividing RFU by OD. Mean and standard deviation of three biological replicates are shown. Statistics were calculated using an ANOVA followed by Tukey-Kramer post hoc test; (***, $P < 0.001$).

Fig. 6. Growth analysis of Δ*nhaR*, *Δhns* and *ΔnhaR*/*Δhns* mutants in M9G 6%NaCl. Cells were grown to OD 0.5 in M9G 1%NaCl and then inoculated into M9G 6%NaCl and growth was measured every hour for 24 h at 37°C. Mean and standard deviation of two biological replicates are shown. Also shown, complementation of Δ*nhaR* with pBA*nhaR*. For all growth curves the area under the curve (AUC) was calculated for each strain and a Student's t-test was performed (**, $P < 0.005$).

Fig. 7. Model of ectoine biosynthesis gene expression in *V. parahaemolyticus*. Solid arrows represent positive regulation while hammer lines represent negative regulation. Previously it was shown that LeuO is required for OmpU expression, an important component of the acid stress response. H-NS was also shown to negatively regulated ToxR. In *E. coli*, NhaR is an activator of NhaA a symporter required for NaCl tolerance. The ? indicates that this has not been shown in *V. parahaemolyticus*. Our data show that the NhaR and LeuO regulate *ectABC-asp_ect* and that H-NS is also part of this regulatory circuit.

499 **References**

500 1. Wood JM. 1999. Osmosensing by bacteria: signals and membrane-based sensors.
501 Microbiol Mol Biol Rev MMBR 63:239-262.
502 2. Poolman B, Glaasker E. 1998. Regulation of compatible solute accumulation in
503 bacteria. Mol Microbiol 29:397-407.
504 3. Galinski EA. 1995. Osmoadaptation in bacteria. Adv Microb Physiol 37:272-328.
505 4. Wood JM. 2011. Bacterial osmoregulation: a paradigm for the study of cellular
506 homeostasis. Annu Rev Microbiol 65:215-38.
507 5. Wood J. 2015. Bacterial responses to osmotic challenges. J Gen Physiol 145: 381-
508 388.
509 6. Csonka L. 1989. Physiological and genetic responses of bacteria to osmotic stress.
510 Microbiol Rev 53: 121-47.
511 7. McLaggan D, Naprstek J, Buurman ET, Epstein W. 1994. Interdependence of K+
512 and glutamate accumulation during osmotic adaptation of *Escherichia coli*. J Biol
513 Chem 269:1911-7.
514 8. da Costa M, Santos H, Galinski E. 1998. An overview of the role and diversity of
515 compatible solutes in Bacteria and Archaea. Ad Biochem Eng/Biotech 61: 117-53.
516 9. Galinski EA, Oren A. 1991. Isolation and structure determination of a novel
517 compatible solute from the moderately halophilic purple sulfur bacterium
518 Ectothiorhodospira marismortui. Eur J Biochem 198:593-8.

519 10. Galinski EA, Pfeiffer HP, Trüper HG. 1985. 1,4,5,6-Tetrahydro-2-methyl-4-
520 pyrimidinecarboxylic acid. A novel cyclic amino acid from halophilic
521 phototrophic bacteria of the genus Ectothiorhodospira. Eur J Biochem 149:135-9.
522 11. Kempf B, Bremer E. 1998. Uptake and synthesis of compatible solutes as
523 microbial stress responses to high-osmolality environments. Arch Microbiol 170:
524 319-30.
525 12. Severin J, Wohlfarth A, Galinski EA 1992. The predominant role of recently
526 discovered tetrahydropyrimidines for the osmoadaptation of halophilic
527 eubacteria. Microbiology 138:1629-1638.
528 13. Czech L, Hermann L, Stöveken N, Richter AA, Höppner A, Smits SHJ, Heider J,
529 Bremer E. 2018. Role of the extremolytes ectoine and hydroxyectoine as stress
530 protectants and nutrients: Genetics, phylogenomics, biochemistry, and structural
531 Analysis. Genes (Basel) 9: 177.
532 14. Hermann L, Mais CN, Czech L, Smits SHJ, Bange G, Bremer E. 2020. The ups and
533 downs of ectoine: structural enzymology of a major microbial stress protectant
534 and versatile nutrient. Biol Chem 401:1443-1468.
535 15. Ongagna-Yhombi SY, Boyd EF. 2013. Biosynthesis of the osmoprotectant ectoine,
536 but not glycine betaine, is critical for survival of osmotically stressed *Vibrio*
537 *parahaemolyticus* cells. Appl Environ Microbiol, 79: 5038-49.

538 16. Pflughoeft KJ, Kierek K, Watnick PI. 2003. Role of ectoine in *Vibrio cholerae*
539 osmoadaptation. Appl Environ Microbiol 69:5919-27.
540 17. Gregory GJ, Morreale DP, Carpenter MR, Kalburge SS, Boyd EF. 2019. Quorum
541 Sensing Regulators AphA and OpaR Control Expression of the Operon
542 Responsible for Biosynthesis of the Compatible Solute Ectoine. Appl Environ
543 Microbiol 85: e01543-19.
544 18. Gregory GJ, Dutta A, Parashar V, Boyd EF. 2020. Investigations of
545 Dimethylglycine, Glycine Betaine, and Ectoine Uptake by a Betaine-Carnitine-
546 Choline Transporter Family Transporter with Diverse Substrate Specificity in
547 Vibrio Species. J Bacteriol 202:e00314-20.
548 19. Naughton LM, Blumerman SL, Carlberg M, Boyd EF. 2009. Osmoadaptation
549 among Vibrio species and unique genomic features and physiological responses
550 of *Vibrio parahaemolyticus*. Appl Environ Microbiol 75:2802-10.
551 20. Graf R, Anzali S, Buenger J, Pfluecker F, Driller H. 2008. The multifunctional role
552 of ectoine as a natural cell protectant. Clin Dermatol 26:326-33.
553 21. Buenger J, Driller H. 2004. Ectoin: an effective natural substance to prevent UVA-
554 induced premature photoaging. Skin Pharmacol Physiol 17:232-7.
555 22. Jebbar M, Talibart R, Gloux K, Bernard T, Blanco C. 1992. Osmoprotection of
556 *Escherichia coli* by ectoine: uptake and accumulation characteristics. J Bact 174:
557 5210-7.

558 23. Sauer T, Galinski EA. 1998. Bacterial milking: A novel bioprocess for production
559 of compatible solutes. Biotechnol Bioeng 57:306-13.
560 24. Czech L, Poehl S, Hub P, Stöveken N, Bremer E. 2018. Tinkering with osmotically
561 controlled transcription allows enhanced production and excretion of ectoine
562 and hydroxyectoine from a microbial cell factory. Appl Environ Microbiol 84:
563 e01772-17.
564 25. Kuhlmann AU, Bremer E. 2002. Osmotically regulated synthesis of the
565 compatible solute ectoine in *Bacillus pasteurii* and related *Bacillus* spp. Appl
566 Environ Microbiol 68:772-83.
567 26. Reshetnikov AS, Khmelenina VN, Trotsenko YA. 2006. Characterization of the
568 ectoine biosynthesis genes of haloalkalotolerant obligate methanotroph
569 "Methylomicrobium alcaliphilum 20Z". Arch Microbiol 184:286-97.
570 27. Louis P, Galinski EA. 1997. Characterization of genes for the biosynthesis of the
571 compatible solute ectoine from Marinococcus halophilus and osmoregulated
572 expression in *Escherichia coli*. Microbiol (Reading) 143:1141-1149.
573 28. Mustakhimov, II, Reshetnikov AS, Fedorov DN, Khmelenina VN, Trotsenko YA.
574 2012. Role of EctR as transcriptional regulator of ectoine biosynthesis genes in
575 Methylophaga thalassica. Biochem (Mosc) 77:857-63.
576 29. Mustakhimov, II, Reshetnikov AS, Khmelenina VN, Trotsenko YA. 2009. EctR--a
577 novel transcriptional regulator of ectoine biosynthesis genes in the

578 haloalcaliphilic methylotrophic bacterium Methylophaga alcalica. Dokl Biochem
579 Biophys 429:305-8.
580 30. Mustakhimov, II, Reshetnikov AS, Glukhov AS, Khmelenina VN, Kalyuzhnaya
581 MG, Trotsenko YA. 2010. Identification and characterization of EctR1, a new
582 transcriptional regulator of the ectoine biosynthesis genes in the halotolerant
583 methanotroph Methylomicrobium alcaliphilum 20Z. J Bacteriol 192:410-7.
584 31. Gregory GJ, Morreale DP, Boyd EF. 2020. CosR is a global regulator of the
585 osmotic stress response with widespread distribution among Bacteria. Appl
586 Environ Microbiol 86:e00120-20.
587 32. Gregory GJ, Boyd EF. 2021. Stressed out: Bacterial response to high salinity using
588 compatible solute biosynthesis and uptake systems, lessons from Vibrionaceae.
589 Comput Struct Biotechnol J 19:1014-1027.
590 33. Shikuma NJ, Davis KR, Fong JN, Yildiz FH. 2013. The transcriptional regulator,
591 CosR, controls compatible solute biosynthesis and transport, motility and biofilm
592 formation in *Vibrio cholerae*. Environ Microbiol 15:1387-99.
593 34. Williams SG, Carmel-Harel O, Manning PA. 1998. A functional homolog of
594 *Escherichia coli* NhaR in *Vibrio cholerae*. J Bacteriol 180:762-5.
595 35. Rahav-Manor O, Carmel O, Karpel R, Taglicht D, Glaser G, Schuldiner S, Padan
596 E. 1992. NhaR, a protein homologous to a family of bacterial regulatory proteins

(LysR), regulates nhaA, the sodium proton antiporter gene in *Escherichia coli*. J Biol Chem 267:10433-8.

36. Król JE. 2018. Regulatory loop between the CsrA system and NhaR, a high salt/high pH regulator. PLoS One 13:e0209554.

37. Pratt LA, Hsing W, Gibson KE, Silhavy TJ. 1996. From acids to osmZ: multiple factors influence synthesis of the OmpF and OmpC porins in *Escherichia coli*. Mol Microbiol 20:911-7.

38. Kenney LJ, Bauer MD, Silhavy TJ. 1995. Phosphorylation-dependent conformational changes in OmpR, an osmoregulatory DNA-binding protein of *Escherichia coli*. Proc Natl Acad Sci U S A 92:8866-70.

39. Chakraborty S, Kenney LJ. 2018. A New Role of OmpR in Acid and Osmotic Stress in Salmonella and E. coli. Front Microbiol 9:2656.

40. Whitaker WB, Parent MA, Boyd A, Richards GP, Boyd EF. 2012. The *Vibrio parahaemolyticus* ToxRS regulator is required for stress tolerance and colonization in a novel orogastric streptomycin-induced adult murine model. Infect Immun 80:1834-45.

41. Gode-Potratz CJ, Chodur DM, McCarter LL. 2010. Calcium and iron regulate swarming and type III secretion in *Vibrio parahaemolyticus*. J Bacteriol 192:6025-38.

615 42. Shimada T, Bridier A, Briandet R, Ishihama A. 2011. Novel roles of LeuO in
616 transcription regulation of E. coli genome: antagonistic interplay with the
617 universal silencer H-NS. Mol Microbiol 82:378-97.
618 43. Navarre WW, McClelland M, Libby SJ, Fang FC. 2007. Silencing of xenogeneic
619 DNA by H-NS-facilitation of lateral gene transfer in bacteria by a defense system
620 that recognizes foreign DNA. Genes Dev 21:1456-71.
621 44. Dorman CJ. 2004. H-NS: a universal regulator for a dynamic genome. Nat Rev
622 Microbiol 2:391-400.
623 45. Dorman CJ. 2007. H-NS, the genome sentinel. Nat Rev Microbiol 5:157-61.
624 46. Lucchini S, Rowley G, Goldberg MD, Hurd D, Harrison M, Hinton JC. 2006. H-
625 NS mediates the silencing of laterally acquired genes in bacteria. PLoS Pathog
626 2:e81.
627 47. Oshima T, Ishikawa S, Kurokawa K, Aiba H, Ogasawara N. 2006. *Escherichia coli*
628 histone-like protein H-NS preferentially binds to horizontally acquired DNA in
629 association with RNA polymerase. DNA Res 13:141-53.
630 48. Hernández-Lucas I, Gallego-Hernández AL, Encarnación S, Fernández-Mora M,
631 Martínez-Batallar AG, Salgado H, Oropeza R, Calva E. 2008. The LysR-type
632 transcriptional regulator LeuO controls expression of several genes in *Salmonella*
633 *enterica* serovar Typhi. J Bacteriol 190:1658-70.

634 49. Shimada T, Yamamoto K, Ishihama A. 2009. Involvement of the leucine response
635 transcription factor LeuO in regulation of the genes for sulfa drug efflux. J
636 Bacteriol 191:4562-71.
637 50. De la Cruz MA, Fernández-Mora M, Guadarrama C, Flores-Valdez MA,
638 Bustamante VH, Vázquez A, Calva E. 2007. LeuO antagonizes H-NS and StpA-
639 dependent repression in Salmonella enterica ompS1. Mol Microbiol 66:727-43.
640 51. Hernández-Lucas I, Calva E. 2012. The coming of age of the LeuO regulator. Mol
641 Microbiol 85:1026-8.
642 52. Ayala JC, Wang H, Benitez JA, Silva AJ. 2018. Molecular basis for the differential
643 expression of the global regulator VieA in *Vibrio cholerae* biotypes directed by H-
644 NS, LeuO and quorum sensing. Mol Microbiol 107:330-343.
645 53. Medina-Aparicio L, Rebollar-Flores JE, Gallego-Hernández AL, Vázquez A,
646 Olvera L, Gutiérrez-Ríos RM, Calva E, Hernández-Lucas I. 2011. The
647 CRISPR/Cas immune system is an operon regulated by LeuO, H-NS, and
648 leucine-responsive regulatory protein in *Salmonella enterica* serovar Typhi. J
649 Bacteriol 193:2396-407.
650 54. Ante VM, Bina XR, Howard MF, Sayeed S, Taylor DL, Bina JE. 2015. *Vibrio*
651 *cholerae leuO* transcription is positively regulated by ToxR and contributes to Bile
652 resistance. J Bacteriol 197:3499-510.

653 55. Bina XR, Howard MF, Ante VM, Bina JE. 2016. *Vibrio cholerae* LeuO links the
654 ToxR regulon to expression of Lipid A remodeling genes. Infect Immun 84:3161-
655 3171.
656 56. Ongagna-Yhombi SY, McDonald ND, Boyd EF. 2015. Deciphering the role of
657 multiple betaine-carnitine-choline transporters in the Halophile *Vibrio*
658 *parahaemolyticus*. Appl Environ Microbiol 81:351-63.
659 57. Oren A. 1999. Bioenergetic aspects of halophilism. Microbiol Mol Biol Rev.
660 63:334-48
661 58. Dover N, Higgins CF, Carmel O, Rimon A, Pinner E, Padan E. 1996. Na+-induced
662 transcription of *nhaA*, which encodes an Na+/H+ antiporter in *Escherichia coli*, is
663 positively regulated by nhaR and affected by hns. J Bacteriol 178:6508-17.
664 59. Dover N, Padan E. 2001. Transcription of nhaA, the main Na(+)/H(+) antiporter
665 of *Escherichia coli*, is regulated by Na(+) and growth phase. J Bacteriol 183:644-53.
666 60. Padan E, Gerchman Y, Rimon A, Rothman A, Dover N, Carmel-Harel O. 1999.
667 The molecular mechanism of regulation of the NhaA Na+/H+ antiporter of
668 *Escherichia coli*, a key transporter in the adaptation to Na+ and H+. Novartis
669 Found Symp 221:183-96.
670 61. Toesca I, Perard C, Bouvier J, Gutierrez C, Conter A. 2001. The transcriptional
671 activator NhaR is responsible for the osmotic induction of osmC(p1), a promoter

672 of the stress-inducible gene osmC in *Escherichia coli*. Microbiology (Reading)
673 147:2795-2803.
674 62. Carmel O, Rahav-Manor O, Dover N, Shaanan B, Padan E. 1997. The Na+-specific
675 interaction between the LysR-type regulator, NhaR, and the *nhaA* gene encoding
676 the Na+/H+ antiporter of *Escherichia coli*. Embo j 16:5922-9.
677 63. Fang M, Majumder A, Tsai KJ, Wu HY. 2000. ppGpp-dependent *leuO* expression
678 in bacteria under stress. Biochem Biophys Res Commun 276:64-70.
679 64. Hertzberg KM, Gemmill R, Jones J, Calvo JM. 1980. Cloning of an EcoRI-
680 generated fragment of the leucine operon of *Salmonella typhimurium*. Gene 8:135-
681 52.
682 65. Dillon SC, Espinosa E, Hokamp K, Ussery DW, Casadesús J, Dorman CJ. 2012.
683 LeuO is a global regulator of gene expression in *Salmonella enterica* serovar
684 Typhimurium. Mol Microbiol 85:1072-89.
685 66. Navarre WW, Porwollik S, Wang Y, McClelland M, Rosen H, Libby SJ, Fang FC.
686 2006. Selective silencing of foreign DNA with low GC content by the H-NS
687 protein in *Salmonella*. Science 313:236-8.
688 67. Park NY, Kim IH, Wen Y, Lee KW, Lee S, Kim JA, Jung KH, Lee KH, Kim KS.
689 2019. Multi-Factor regulation of the master modulator LeuO for the Cyclic-(Phe-
690 Pro) signaling pathway in *Vibrio vulnificus*. Sci Rep 9:20135.

691 68. Park NY, Lee KW, Kim KS. 2020. H-NS Silences Gene Expression of LeuO, the
692 Master Regulator of the Cyclic(Phe-Pro)-dependent Signal Pathway, in *Vibrio*
693 *vulnificus*. J Microbiol Biotechnol 30:830-838.
694 69. Makino K, Oshima K, Kurokawa K, Yokoyama K, Uda T, Tagomori K, Iijima Y,
695 Najima M, Nakano M, Yamashita A, Kubota Y, Kimura S, Yasunaga T, Honda T,
696 Shinagawa H, Hattori M, Iida T. 2003. Genome sequence of *Vibrio*
697 *parahaemolyticus*: a pathogenic mechanism distinct from that of V cholerae. Lancet
698 361:743-9.
699 70. Whitaker WB, Parent MA, Naughton LM, Richards GP, Blumerman SL, Boyd EF.
700 2010. Modulation of Responses of *Vibrio parahaemolyticus* O3:K6 to pH and
701 Temperature Stresses by Growth at Different Salt Concentrations. Appl Environ
702 Microbiol, 76: 4720-9.
703 71. Dehio C, Meyer M. 1997. Maintenance of broad-host-range incompatibility group
704 P and group Q plasmids and transposition of Tn5 in Bartonella henselae
705 following conjugal plasmid transfer from *Escherichia coli*. J Bacteriol 179:538-40.
706 72. Jutras BL, Verma A, Stevenson B. 2012. Identification of novel DNA-binding
707 proteins using DNA-affinity chromatography/pull down. Curr Protoc Microbiol
708 Chapt 1:F.1.

709 73. Chaparian RR, Olney SG, Hustmyer CM, Rowe-Magnus DA, van Kessel JC. 2016.
710 Integration host factor and LuxR synergistically bind DNA to coactivate quorum-
711 sensing genes in Vibrio harveyi. Mol Microbiol 101:823-40.
712 74. Tague JG, Hong J, Kalburge SS, Boyd EF. 2022. Regulatory Small RNA Qrr2 Is
713 Expressed Independently of Sigma Factor-54 and Can Function as the Sole Qrr
714 Small RNA To Control Quorum Sensing in *Vibrio parahaemolyticus*. J Bacteriol
715 204:e0035021.
716 75. Jutras BL, Liu Z, Brissette CA. 2010. Simultaneous isolation of Ixodidae and
717 bacterial (*Borrelia* spp.) genomic DNA. Curr Protoc Microbiol Chapt 1:E.2.
718 76. Tague JG, Regmi A, Gregory GJ, Boyd EF. 2021. Fis connects two sensory
719 pathways, quorum sensing and surface sensing, to control motility in *Vibrio*
720 *parahaemolyticus*. Front Microbiol 12:669447.
721 77. Gibson DG. 2011. Enzymatic assembly of overlapping DNA fragments. Methods
722 Enzymol 498:349-61.
723 78. Philippe N, Alcaraz JP, Coursange E, Geiselmann J, Schneider D. 2004.
724 Improvement of pCVD442, a suicide plasmid for gene allele exchange in bacteria.
725 Plasmid 51:246-55.
726 79. Horton RM, Hunt HD, Ho SN, Pullen JK, Pease LR. 1989. Engineering hybrid
727 genes without the use of restriction enzymes: gene splicing by overlap extension.
728 Gene 77:61-8.

80. Karunakaran R, Mauchline TH, Hosie AHF, Poole PS. 2005. A family of promoter probe vectors incorporating autofluorescent and chromogenic reporter proteins for studying gene expression in Gram-negative bacteria. Microbiol (Reading) 151:3249-3256.

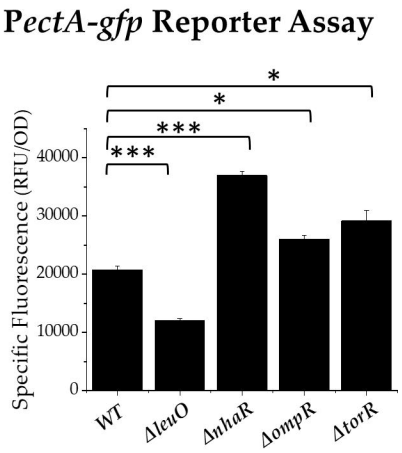
PectA-gfp Reporter Assay
Specific Fluorescence (RFU/OD)
0
10000
20000
30000
40000
***
***
*
*
WT
ΔleuO
ΔnhaR
ΔompR
ΔtorR

Fig. 1

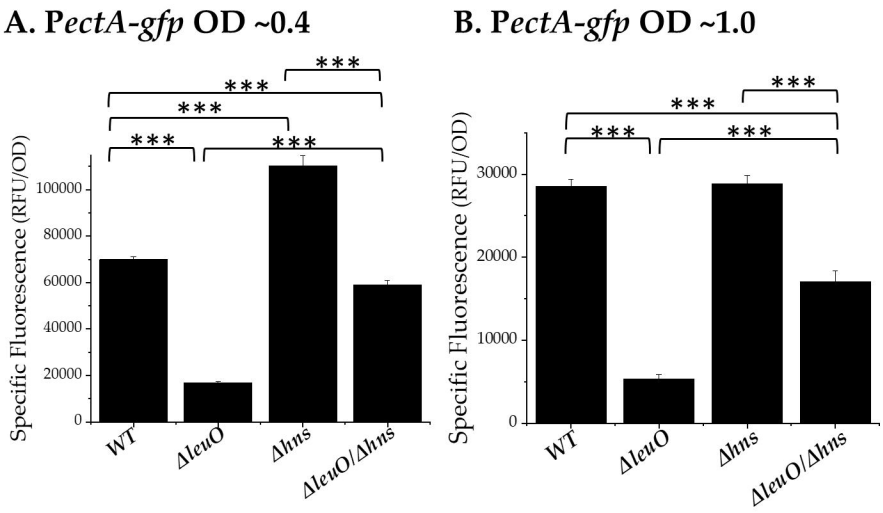
A. PectA-gfp OD ~0.4
B. PectA-gfp OD ~1.0
Specific Fluorescence (RFU/OD)
***
WT
ΔleuO
Δhns
ΔleuO/Δhns
0
20000
40000
60000
80000
100000
10000
30000

Fig. 2

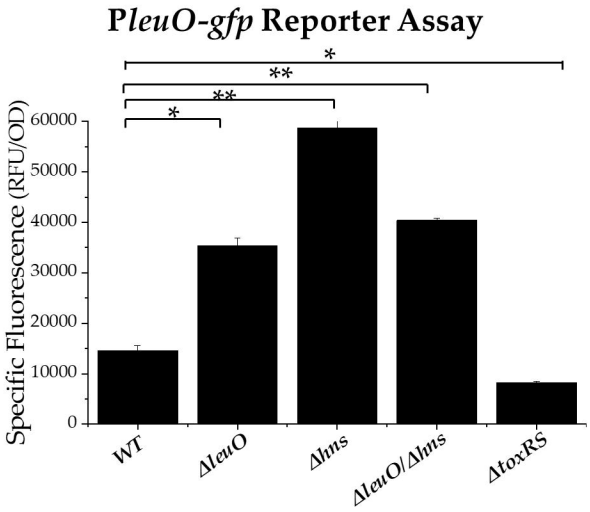
PleuO-gfp Reporter Assay
Specific Fluorescence (RFU/OD)
60000
50000
40000
30000
20000
10000
0
*
**
**
*
WT
ΔleuO
Δhns
ΔleuO/Δhns
ΔtoxRS

Fig. 3

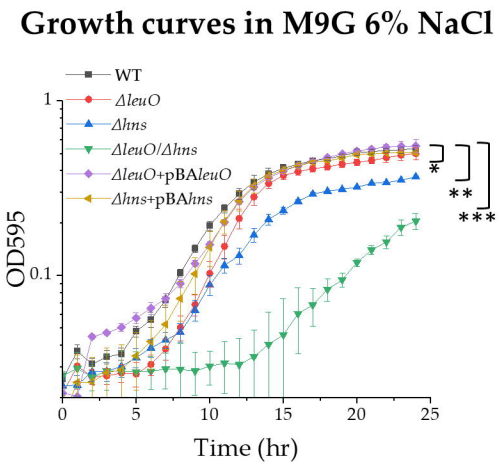
Growth curves in M9G 6% NaCl
WT
ΔleuO
Δhns
ΔleuO/Δhns
ΔleuO+pBAleuO
Δhns+pBAhns
OD595
1
0.1
0
5
10
15
20
25
Time (hr)
*
**
***

Fig. 4

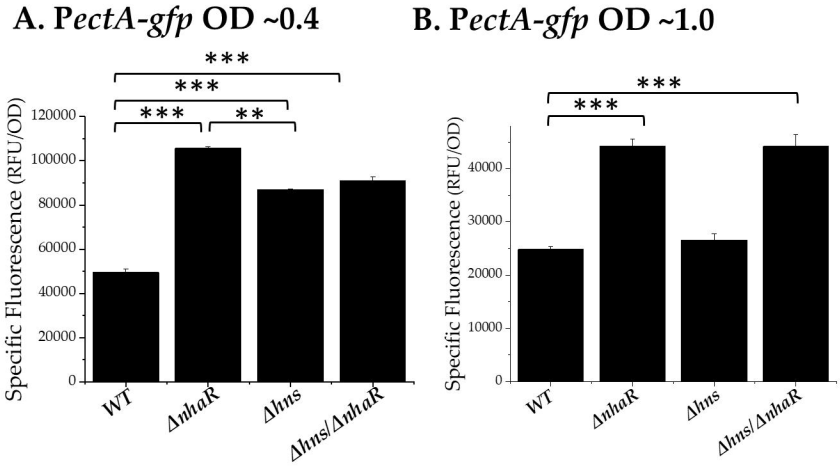
A. PectA-gfp OD ~0.4
B. PectA-gfp OD ~1.0
Specific Fluorescence (RFU/OD)
***
**
WT
ΔnhaR
Δhns
Δhns/ΔnhaR

Fig. 5

Growth curves in M9G 6% NaCl

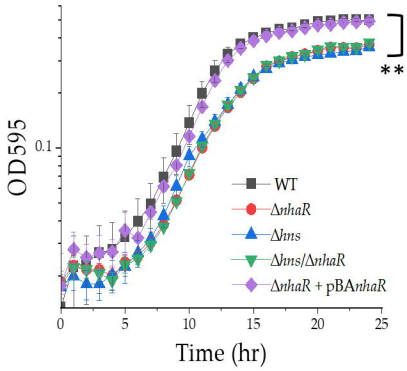

Fig. 6

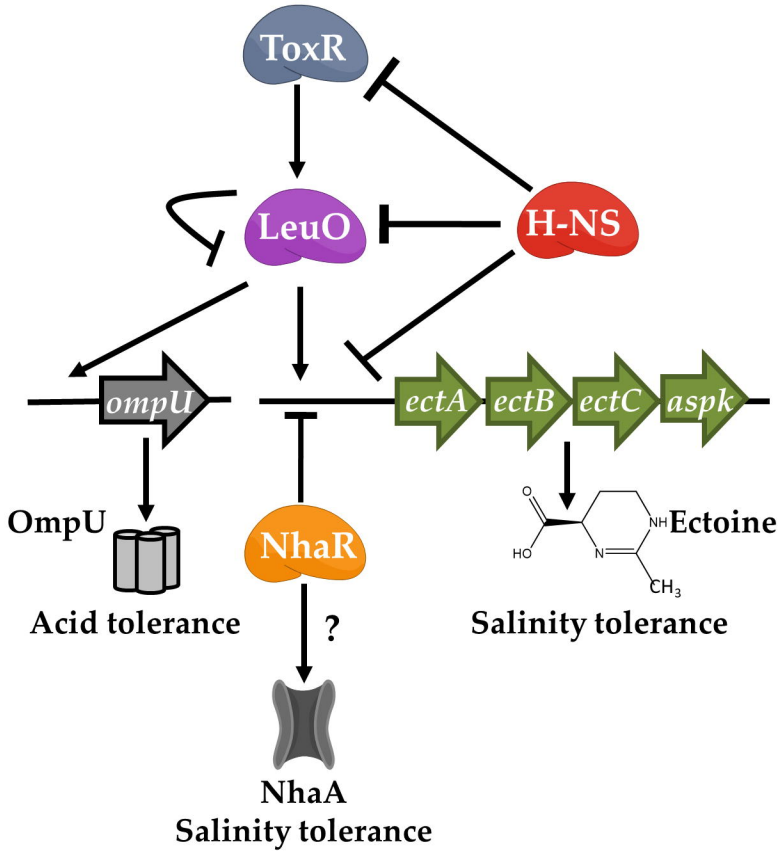
ToxR
LeuO
H-NS
ompU
ectA
ectB
ectC
aspk
OmpU
Acid tolerance
NhaR
?
NhaA
Salinity tolerance
Ectoine
Salinity tolerance

Fig. 7